Preparation of benzocyclobutene-functionalized organic-inorganic hybrid microspheres and their reduction of permittivity to DVSBCB resin

Qiuxia Peng[*a], Jiajun Ma[b], Ji Wu[a], Ruichao Chen[c], Zejun Pu[a], Jiachun Zhong[a], Junxiao Yang[*b]

[a] Sichuan University of Science & Engineering, Zigong, 643000, China

[b] State Key Laboratory of Environmental-friendly Energy Materials, Southwest University of Science and Technology, Mianyang, 62010, China.

[c] School of Electronic Science and Engineering, University of Electronic Science and Technology of China, Chengdu, 611731, China

[*] Corresponding author

(Email: Qiuxia Peng: pengqiuxia2013@163.com; Junxiao Yang: yangjunxiao@swust.edu.cn)

This document contains the following supporting information:

➢ Fig. S1. (a) ^{13}C NMR and (b) ^{1}H NMR spectra of BCBVST.

➢ Fig. S2. DLS curve of BMPS;

➢ Fig. S3. SEM images of BMPS;

➢ Fig. S4. SEM images of Series 1-4;

➢ Table S1. Information on the filler used for the control experiments.

➢ Fig. S5. Hardness and Young's modulus vs. depth of penetration;

➢ Fig. S6. Loading and unloading curves for the cured composite material;

➢ Fig. S7. TG-DSC curves of BMPS;

➢ Fig. S8. TEM images of BMPS;

➢ Fig. S9. TG curves of the pure matrix and composite material;

➢ Fig. S10. CTE curves of matrix and composite material after curing;

➢ Fig. S11. Curves of the dielectric constant of LSOVBCB resin and

BMPS/LSOVBCB composite as a function of frequency;
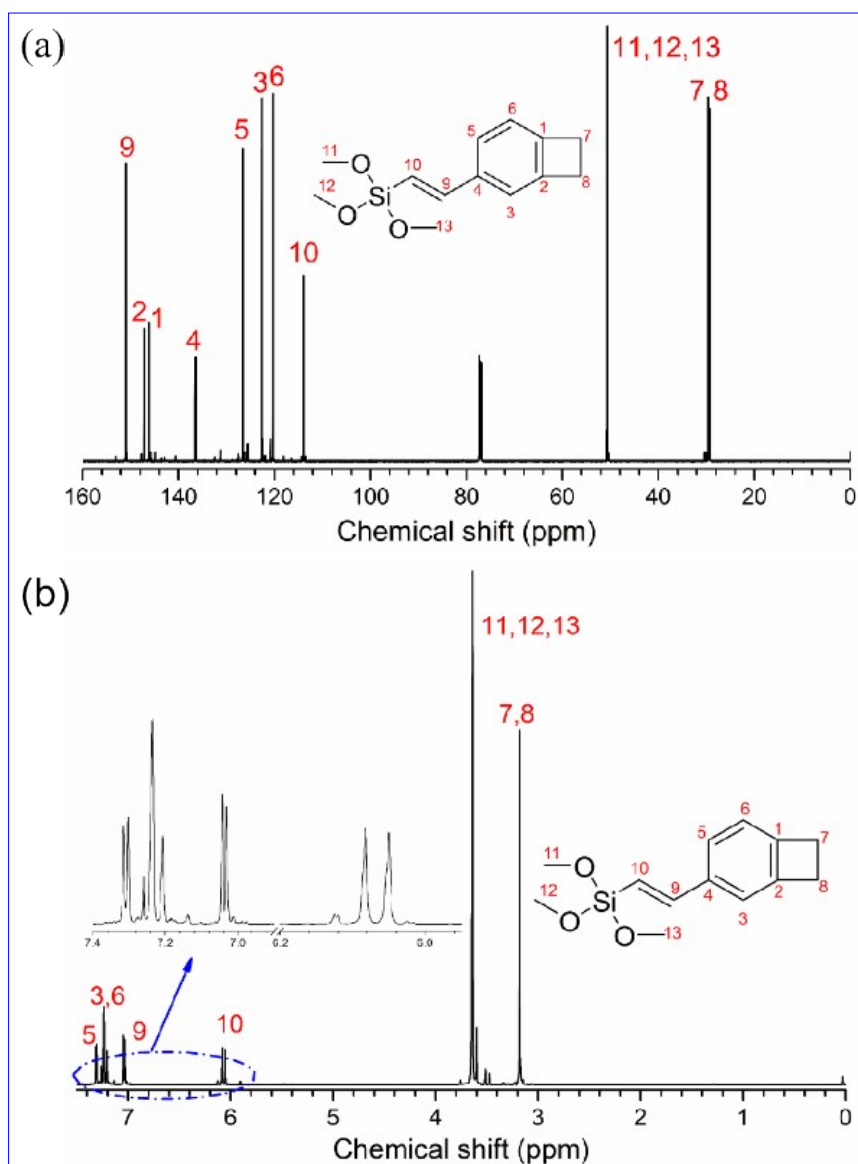
Fig. S1. (a) ^{13}C NMR and (b) ^{1}H NMR spectra of BCBVST.
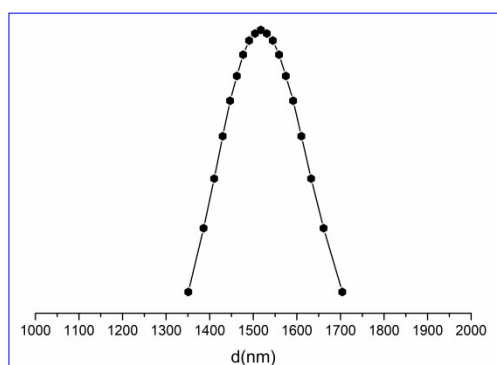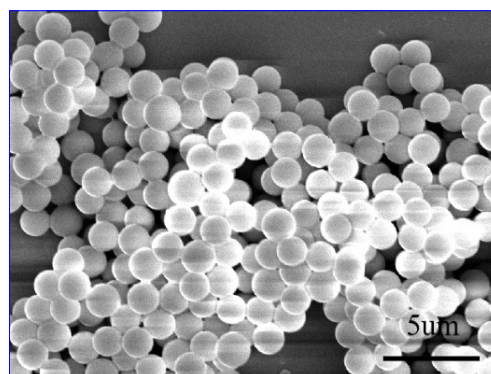

Fig.S2. DLS curve of BMPS.
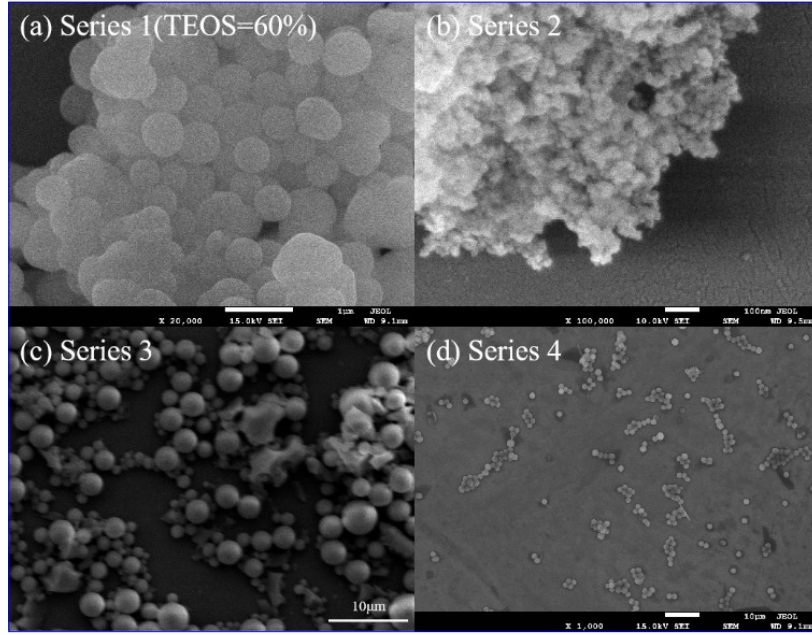

Fig. S3. SEM image of BMPS.

Fig. S4. SEM images of (a) Series 1 (BCBVST: TEOS=2:3, the scale is 1 μm); (b) Series 2 (BCBVST@SiO₂, the scale is 100 nm); (c) Series 3 (VTEOS, the scale is 10 μm); (d) Series 4 (BCBVST-cured, the scale is 10 μm).

Table S1. Information on the filler used for the control experiments.

filler	name	Preparation method	The purpose of preparing the filler
Series 1	BTMPS	BCBVST is co-hydrolyzed with TEOS, where the mass fraction of TEOS ranges from 20% to 80%.	To study the effect of the percentage of BCB group and inorganic component in filler on its dispersibility in DVSBCB resin.
Series 2	BCBVST@SiO₂	nano-SiO₂ surface modified by BCBVST	Study the effect of surface BCB groups on the dispersion of fillers in DVSBCB resin.
Series 3	VTEOS	The hydrolyzed product of vinyl triethoxy silane, there is abundant vinyl on the surface.	Study the reaction between the difference of filler surface groups and DVSBCB resin.
Series 4	BMPS-cured	The BCB group of BMPS has been inactivated by heat treatment.	Study the effect of BCB group activity on the compatibility of BMPS with DVSBCB resin.

The hardness and Young's modulus of the composite film were measured by nanoindentation analysis. The continuous stiffness model was used to obtain the

loading curves at multiple test points as a function of indentation depth (see Fig. S5) and the curves of hardness and modulus were obtained at individual points as a function of indentation depth (see Fig. S6). The loading and unloading results from five different points in the composite material are similar, indicating that the film sample has uniform mechanical properties at all points in the horizontal direction. Furthermore, the hardness and modulus for a single point do not change significantly with indentation depth, indicating that the surface and interior of the sample are uniform. These results indicate that the microspheres are uniformly dispersed in the matrix and have good compatibility and adhesion with the matrix.
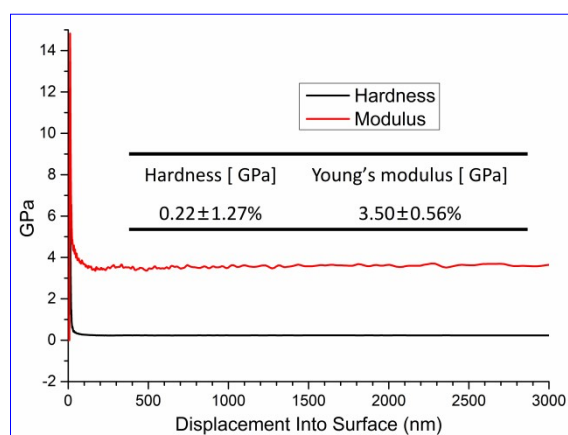

Fig. S5. Hardness and Young's modulus vs. depth of penetration of the cured composite material.
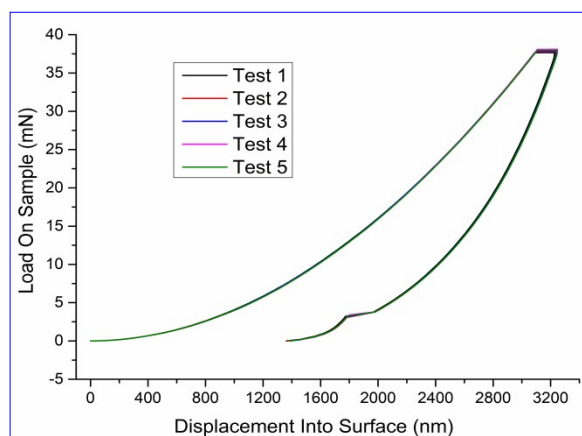

Fig. S6. Loading and unloading curves of the cured composite material.

The DSC curve (Fig. S7) shows that the BMPS exhibits a small amount of heat absorption at 170 °C and a large amount of heat release at 250 °C. Correspondingly, TGA of BMPS shows that ~3% weight loss occurs below 200 °C, which is caused by

the incomplete condensation of Si–OH or Si–OCH$_3$ remaining in the microspheres. They condense further under heat (endothermic reaction), releasing small molecules such as water or alcohols. Subsequently, with the increase of temperature, the four-membered ring in BCB undergoes ring-opening crosslinking (exothermic reaction), and the degree of crosslinking of the system increases. Therefore, the temperature for the further weight loss of 5% (i.e., an overall weight loss of ~8%) exceeds 500 ℃.
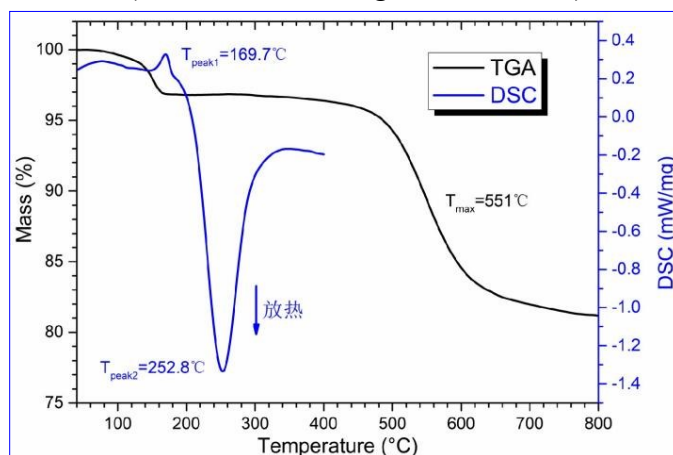

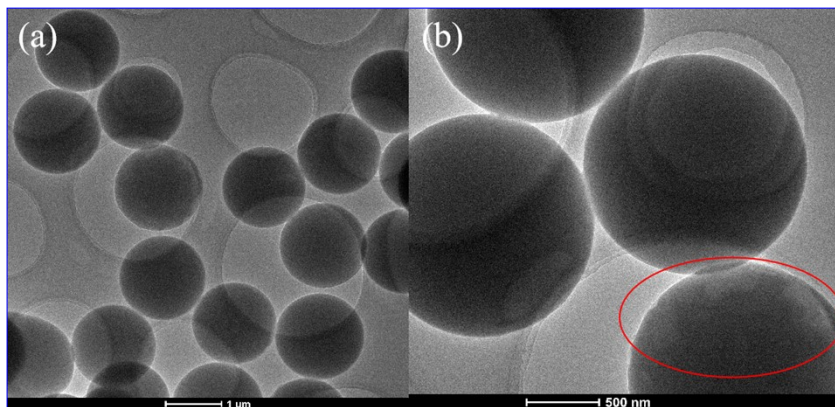
Fig. S7. The TG and DSC curves for BMPS.

Fig. S8. TEM images of BMPS.

The thermal stability of the matrix was evaluated by measuring the temperature at 5 wt% weight loss (T_5) and the temperature at maximum degradation rate (T_{max}) of the composite under a nitrogen atmosphere, from 30 to 800 ℃ at a rate of 10 ℃/min. The results were compared with those obtained for the matrix without BMPS (Fig. S8), in

order to assess the impact of BMPS on thermal stability. Theoretically, the cage/ladder structure of BMPS is beneficial for improving the thermal stability of the composites. However, according to the results of TG, the addition of BMPS may be due to the small amount, so it seems to be helpful to the thermal stability of the composite, but the effect is not significant.
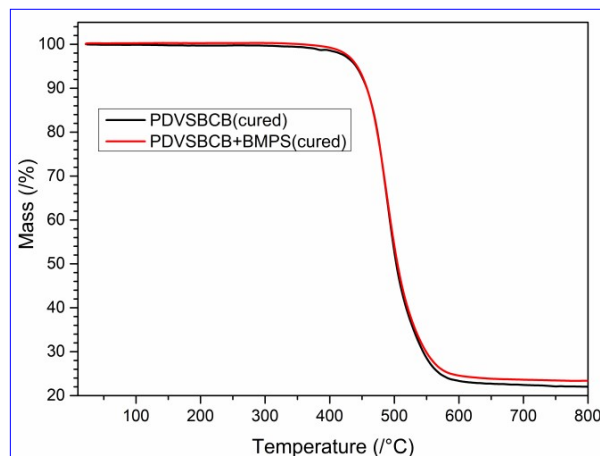

Fig. S9. TG curves of the pure matrix (PDVSBCB) and composite material (BMPS/PDVSBCB).

In addition, the CTE (Fig. S9) of the composite material does not change significantly compared with that of the matrix in the room temperature to 350 °C range. These results indicate that the introduction of the filler has no adverse effects on the thermal stability of the matrix.
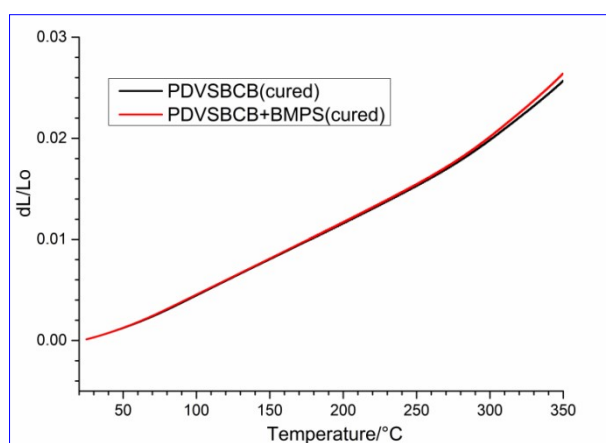

Fig. S10. CTE curves of PDVSBSB-cured and composite material (PDVSBSB+BMPS)-cured.
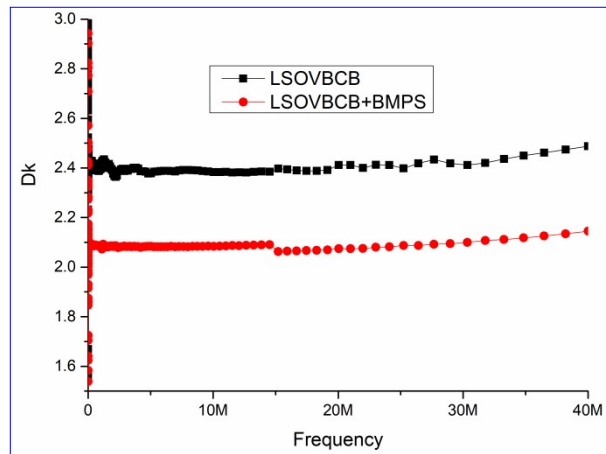
Fig. S11. Curves of the dielectric constant of LSOVBCB resin and BMPS/LSOVBCB composite as a function of frequency
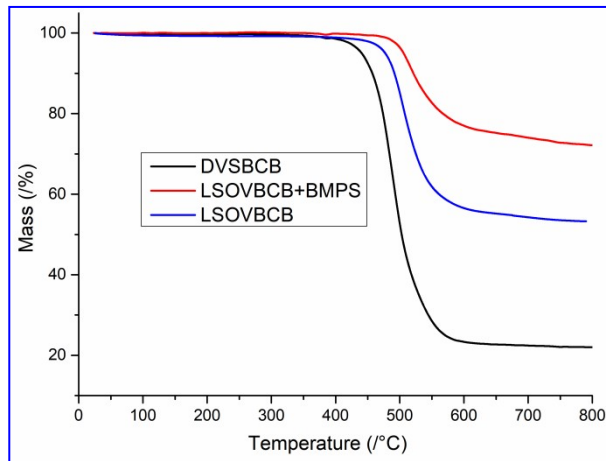

Fig. S12. TG curves of LSOVBCB and its composites